ES Food and Agroforestry
DOI: https://dx.doi.org/10.30919/faf2196

Synthesis of Biogenic Manganese Oxide Nanoparticles from Wheat Bagasse and Their Applications in Biological and Dye Degradation Potential

Amrish Kumar,[1] Amanpreet Kaur,[1,*] Man Vir Singh,[2] Shubhangee Agarwal,[1] Shobhna Mishra[3] and Sheetal Tyagi[4]

Abstract

Interest in biogenic nanoparticles derived from plant waste has increased due to the growing demand for environmentally friendly and sustainable nanomaterials. A green synthesis method was employed in this work to create manganese oxide nanoparticles (MnO NPs) using wheat bagasse extract as a natural reducing and stabilizing agent. Some advanced analytical techniques, like Fourier-transform infrared spectroscopy (FTIR), X-ray diffraction (XRD), and field emission scanning electron microscopy, were used to validate the size, shape, morphological, and structural properties of synthesized nanoparticles. The successful synthesis of MnO NPs was confirmed by UV-Vis spectroscopy, which demonstrated a clear peak at 329 and 376 nm. Phytoconstituents functioning as capping agents were identified by FTIR, which showed absorption bands. Morphological information was obtained using FESEM, and a crystalline size of 38.51 nm was found using XRD examination, calculated by the Debye-Scherrer equation. The Congo red deterioration under visible light irradiation was utilized to assess the photocatalytic efficacy of MnO NPs and validate their suitability for environmental cleanup. Antioxidant potential was evaluated using the DPPH and ABTS radical scavenging tests, which produced IC_{50} values of 30.34 µg/mL and 34.45 µg/mL, respectively. When evaluating antibacterial activity against bacteria, substantial inhibitory effects were found. All of the bacterial strains under investigation showed a strong, dose-dependent inhibitory action with sizable zones of inhibition. Additionally, the α-amylase and α-glucosidase inhibition tests showed promising antidiabetic effects, with IC_{50} values of 256.45 µg/mL and 215.76 µg/mL, respectively. These results imply that MnO NPs made from wheat bagasse provide a viable platform for environmental and medicinal uses.

Keywords: Agriculture waste; MnO; Nanoparticles; Antibacterial; Photocatalytic potential.
Received: 07 January 2026; Revised: 17 March 2026; Accepted: 25 April 2026
Article type: Research article.

1. Introduction

The area of nanotechnology has grown in importance, providing creative answers for a wide range of scientific and industrial domains, such as environmental remediation, agriculture, and medicine. Metal oxide nanoparticles have attracted considerable attention owing to their distinctive physicochemical characteristics, large surface area, adjustable reactivity, and electrical adaptability,[1] in particular because of their intrinsic redox activity, environmental friendliness, and biocompatibility. MnO NPs (Nanoparticles) have become attractive options for use in energy storage, biosensing, catalysis, and biomedical sciences.[2] Chemical or physical techniques, including sol-gel processing, hydrothermal treatment, or thermal breakdown, are often used in the conventional production of MnO nanoparticles. Although these methods often produce well-defined nanostructures, they have many disadvantages, like the utilization of hazardous compounds, high energy requirements, and the generation of poisonous byproducts.[3] These restrictions have sparked interest in new, environmentally friendly, sustainable synthesis methods that preserve scalability and efficiency while reducing their negative effects on the environment.[4] Utilising biological systems like plant extracts, microbes, or bio-wastes, biogenic or green synthesis techniques have become appealing substitutes.[5] In particular, biomaterials generated from plants provide an easy and environmentally acceptable substrate for the production of nanoparticles. They have a wide variety of phytoconstituents functioning as organic stabilising and

[1]*Department of Chemistry, School of Sciences, IFTM University, Moradabad, Uttar Pradesh, 244102, India*
[2]*Department of Chemistry, Graphic Era (Deemed to be University), Dehradun, Uttarakhand, 248002, India*

reducing agents, including tannins, alkaloids, flavonoids, and phenolics.[6] Among the several plant-based substrates, wheat bagasse and other agricultural leftovers are inexpensive, renewable, and underutilised resources. With the help of bioactive substances and lignocellulosic material, wheat bagasse, the fibrous waste left over after juice extraction or milling, can efficiently facilitate the production of nanoparticles without the need for additional chemicals.[7] Manganese oxide nanoparticles synthesised by environmentally friendly methods utilising wheat bagasse have shown a variety of biological functions. Because of their antioxidant properties, they may scavenge reactive oxygen species (ROS), preserving biological systems from oxidative stress-related damage.[8] Furthermore, MnO nanoparticles exhibit potent antibacterial activity against bacteria, most probably by processes that include oxidative stress production and membrane disruption.[9] Additionally, their possible antidiabetic effects, which are ascribed to the inhibition of important enzymes like α-amylase and α-glucosidase, indicate their therapeutic value in the treatment of hyperglycemia.[10] Apart from its application in biomedicine, MnO NPs have demonstrated catalytic efficacy in the breakdown of synthetic dyes, which are persistent pollutants present in industrial wastewater. Their ability to accelerate dye breakdown in mild conditions highlights their potential for environmental remediation.[11]

In this study, an environmentally friendly, one-pot synthesis technique was used to create manganese oxide nanoparticles using wheat bagasse extract. Advanced analytical methods were used to evaluate the structural and morphological characteristics of the synthesised nanoparticles. Together with their catalytic capability in dye degradation, their antibacterial, antidiabetic, and antioxidant properties were thoroughly assessed. In addition to showing a sustainable method for creating nanoparticles, this study emphasises the versatility of MnO nanoparticles made from wheat bagasse for both environmental and medicinal uses.

2.Method and material

2.1 Material

Wheat bagasse was collected from local agricultural farms in a clean, dry state and stored at room temperature until use. Manganese sulphate monohydrate ($MnSO_4 \cdot H_2O$), used as the precursor salt for nanoparticle synthesis, was acquired from Sigma-Aldrich (USA). All reagents and compounds, including p-nitrophenyl-α-D-glucopyranoside (pNPG), congo red, were of analytical quality and obtained. Microbial strains used for the antibacterial study were procured from a certified microbial culture collection center. Nutrient agar and Mueller-Hinton agar used for bacterial culture and antimicrobial testing were purchased from HiMedia. Sterile Petri dishes, micropipettes, culture tubes, and other microbiological lab consumables were used as required. All glassware was sterilized before use, and deionized water was utilized in all experimental preparations.

2.2 Preparation of wheat bagasse extract

Dried wheat bagasse was pulverised into a fine powder utilising a mechanical grinder. Approximately 10 g of the powder was subjected to 500 mL of ethanol for extraction. The mixture was then cooled and filtered with Whatman No. 1 filter paper. The filtrate was preserved at 4 °C and utilised as the reducing and stabilizing agent for the synthesis of manganese oxide nanoparticle.[12]

2.3 Phytochemical analysis

A preliminary analysis of the phytochemical content of wheat bagasse extract was executed to ascertain the main bioactive components responsible for stabilising and reducing MnO NPs. In order to identify several secondary metabolites, standard qualitative phytochemical experiments were conducted.[13] The extract yielded positive results, revealing the presence of flavonoids, phenolic compounds, alkaloids, saponins, and tannins. Because of their potent reducing and antioxidant qualities, flavonoids and phenolic chemicals are thought to be essential for the production and capping of MnO NPs. On the other hand, alkaloids and saponins could support the stability and biological nanoparticle activity. In addition to potentially influencing the dimensions and morphology of the nanoparticles, the presence of tannins and terpenoids enhances the extract's reducing activity.[14]

2.4 Synthesis of MnO nanoparticles

Throughout the synthesis of manganese oxide nanoparticles, 50 millilitres of a homogenous solution of 0.01 M manganese sulphate monohydrate ($MnSO_4 \cdot H_2O$) and 50 millilitres of wheat bagasse extract were combined in a conical flask, and then the reaction mixture underwent continuous stirring between 60 and 70 °C for two hours. The development of MnO nanoparticles and the decrease of Mn2+ ions are demonstrated by the dark brown color that appears throughout the process. The mixture was left at ambient temperature for a full day to allow the nanoparticles to properly nucleate and mature.[15]

To extract the nanoparticle pellet, the outcome Centrifugation was conducted for a duration of 15 minutes at a speed of 10,000 rpm. The pellet underwent multiple purification processes using distilled water and ethanol to eliminate contaminants and unbound phytochemicals. Following a drying process at 60 °C in a hot air oven, the purified nanoparticles underwent calcination for two hours at 400 °C to yield phase-pure manganese oxide and enhance crystallinity. This green synthesis technique offers a scalable, reasonably priced, and environmentally safe means of producing functional metal oxide nanoparticles that could be

[3]*Department of Home Science, Jamuna Prasad Memorial College, Bhairpura, Bareilly, Uttar Pradesh, 243202, India*
[4]*Department of Chemistry, School of Basic and Applied Sciences, Shri Guru Raam Rai University, Dehradun, Uttarakhand, 248001, India*
[*]*Email:* amanpreet2225@gmail.com (A. Kaur)

applied to biomedicine and environmental remediation by utilizing the natural reducing power of agricultural waste.[16]

2.5 Statistical analysis

All experiments were performed in triplicate, and the results were described using mean ± standard deviation (SD). GraphPad Prism (version X) and a comparable statistical software program were employed to carry out the statistical analysis. The significance of variations among treatment groups was assessed through Tukey's post hoc test following a one-way ANOVA. P-values below 0.05 were considered statistically significant. The trends in the manganese oxide nanoparticles' antioxidant, antibacterial, anti-diabetic, and photocatalytic activity were plotted on graphs. Where appropriate, correlation analysis was also conducted to evaluate the connection between biological activity and nanoparticle concentration.

3. Results

3.1 Extraction and phytochemical analysis

A yield of 6.14% was obtained by extracting the wheat bagasse material using an ethanol solvent. To determine the different phytochemical components that aid in the stabilisation and reduction of MnO NPs, the extract was subjected to qualitative analysis. As shown in Table 1, the study revealed that the extract had a significant quantity of secondary metabolites. These substances most likely aid in the process of reducing Mn ions and serve as capping agents, which enhance the stability of nanoparticles by avoiding their clustering.[17] The creation of nanoparticles is especially influenced by polar phytochemicals that are extracted using polar solvents.

3.2 Characterization of MnO nanoparticles

3.2.1 UV−VIS spectroscopy

Using UV-visible spectroscopy, the optical characteristics and initial validation of manganese oxide (MnO) nanoparticle production were evaluated. A UV–Vis spectrophotometer (Shimadzu UV-1800) was used to do the analysis. From the UV experiments, two prominent peaks at 329 and 376 nm were observed, which reveal the synthesis of MnO nanoparticles and indicate effective biogenesis (Fig. 1). The inherent band gap transition of MnO nanoparticles is shown through the absorption band at 329 nm, suggesting the existence of nanocrystalline characteristics of MnO.[18]

The presence of surface-bound phytochemicals derived from the wheat extract could be responsible for the peak observed at 376 nm, potentially influencing the optical behaviour of the nanoparticles.[19] The development of stable, evenly distributed MnO nanoparticles with no agglomeration is suggested by the existence of these peaks without any discernible absorption beyond 400 nm. These findings confirm the efficacy of wheat utilised as a capping agent in the eco-friendly production of MnO nanoparticles.

3.2.2 FTIR analysis

The functional groups involved in the reduction and stability processes were identified through the analysis of the FTIR spectra of the synthesised MnO nanoparticles (MnO NPs) and wheat bagasse. The investigation confirmed that the resultant nanoparticle product contained phytochemical constituents and that Mn–O bonds were established. FTIR spectra were collected within the spectral range of 4000–400 cm^{-1}, utilising a resolution of 4 cm. A background spectrum of pure KBr was recorded before the analysis of the sample and subsequently subtracted from the sample spectra to remove background noise.[20] The wheat bagasse spectrum exhibited notable absorption bands at 3682 cm^{-1} and 3376 cm^{-1}, suggesting the presence of polyphenols and alcohols, which are associated with the O–H stretching vibrations of hydroxyl groups. The peaks observed at 2905 cm^{-1} can be attributed to the C–H stretching vibrations of aliphatic chains. The band observed at 1298 cm^{-1} corresponds to the C–N stretching of amines, while the bands at 1635 cm^{-1} is attributed to C=O stretching and aromatic C=C stretching, respectively.

The presence of polysaccharides and other macromolecules is suggested by the strong bands that span from 995 cm^{-1} to 520 cm^{-1}. On the other hand, MnO NPs' FTIR spectra showed a shift and a decrease in the strength of a number of bands, suggesting that phytochemicals and manganese ions successfully interacted during the creation of the nanoparticles.

Observations indicate peaks at 1643 cm^{-1} indicate preserved organic moieties on the nanoparticle surface, the large peak at 3355 cm^{-1} reflects residual O–H groups. The creation of manganese oxide nanoparticles is validated by the notable appearance of new peaks at 593 cm^{-1} and 583 cm^{-1}, which are typical of Mn–O stretching vibrations. The FTIR spectra are shown in Fig. 2. Numerous functional group peaks in the wheat bagasse spectrum have shifted or vanished, which shows that they are engaged in the reduction and capping processes.[21]

3.2.3 XRD analysis

To evaluate the crystallinity and phase purity of the nanoparticle's diffraction patterns were captured.[22] This method demonstrated the nanoparticles' crystalline nature and average crystallite size, which is crucial for understanding their potential applications across a range of fields. The crystal form, phase purity, and particle size of the synthesised material manganese oxide (MnO) nanoparticles were assessed by XRD. An X-ray diffractometer (Rigaku Miniflex II) was used to perform XRD. The analysis was done directly using the powdered dry manganese oxide nanoparticles. The crystallite size of the nanoparticles employed the Debye-Scherrer equation, $D = K\lambda/\beta \cos \theta$, where β represents the FWHM and D is the average. It was determined from the above computation that the crystals of manganese oxide particles are in the nano range. The equivalent 2θ value for the (210) diffraction plane was found at 59.7436° with a full width at half maximum (FWHM) of 0.3515°. These diffraction peaks match well with the standard JCPDS card No. 07-0230,

Table 1: Screening of the ethanolic extract of wheat bagasse for qualitative phytochemicals.

Phytoconstituents	Ethanol extract
Alkaloids	-
Flavonoids	+
Phenol	+
Saponins	-
Tannins	-
Triterpenoids	+

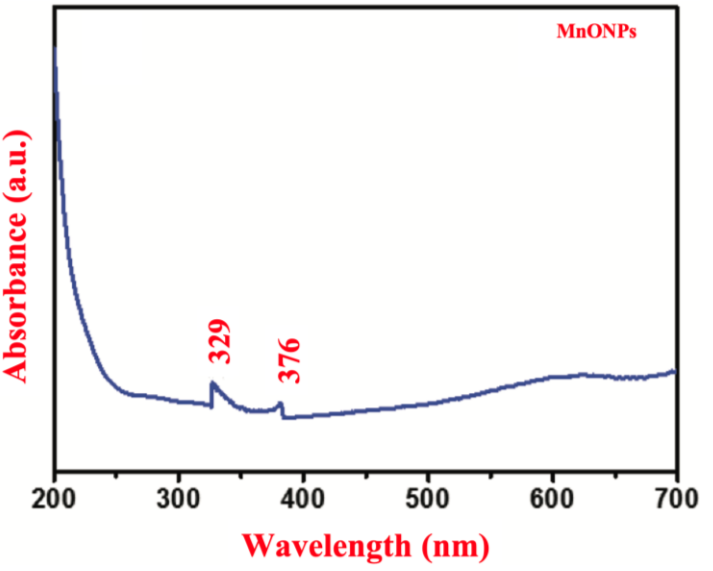

Fig. 1: UV–Vis absorption spectrum of MnO nanoparticles synthesis from wheat bagasse extract.

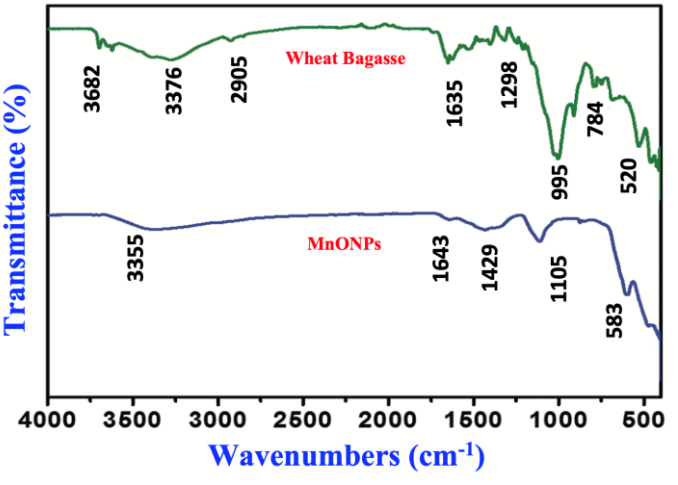

Fig. 2: FTIR spectra of MnO NPs synthesis from wheat bagasse extract.

confirming the formation of phase-pure MnO nanoparticles.

For precise computation, the FWHM was converted to radians, and the Bragg angle (θ) was found to be 29.8718° (Fig. 3). When these numbers were entered into the formula, the crystallite size for the (210) plane came out to be around 38.51 nm.[23] The data has been summarized in Table 2.

3.2.4 FESEM

Another advanced analytical technique, FESEM, was adopted to examine various factors like Surface morphology, particle dimensions, and particle distribution of newly synthesized nano materials using different magnification ranges from 10,000× to 100,000×.[20]

The MnO NPs showed some aggregation and a variety of morphologies, including irregular, granular, and ellipsoidal forms.[24] The MnO NPs' sizes varied from 30 to 50 nm, according to the SEM examination. The microscopic analysis revealed that the nanoparticles were uniformly dispersed throughout the sample and mostly had a spherical shape. The dehydration process that took place during the sample preparation for SEM analysis might be connected to the notable aggregation of the MnONPs. Fig. 4 displays the

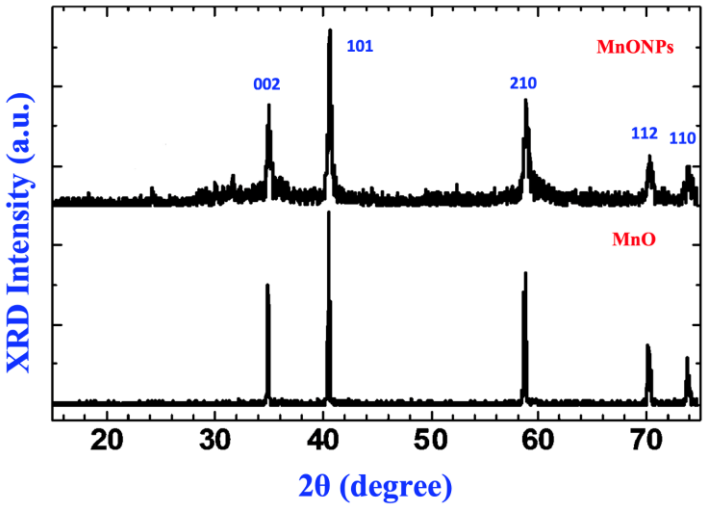

Fig. 3: MnO NPs XRD patterns using wheat bagasse extract.

Table 2: Miller Indices, FWHM values, d-spacing, and average crystallite size calculated for MnO NPs synthesized from wheat bagasse extract.

hkl	Pos. [°2Th.]	FWHM Left [°2Th.]	d-spacing [Å]
002	35.3568	0.3453	2.54543
101	41.8754	0.5715	2.69480
210	59.7436	0.3515	2.14353
122	71.3973	0.3054	1.95754
110	74.6270	0.2494	1.86654
Average crystallite size 38.51nm.			

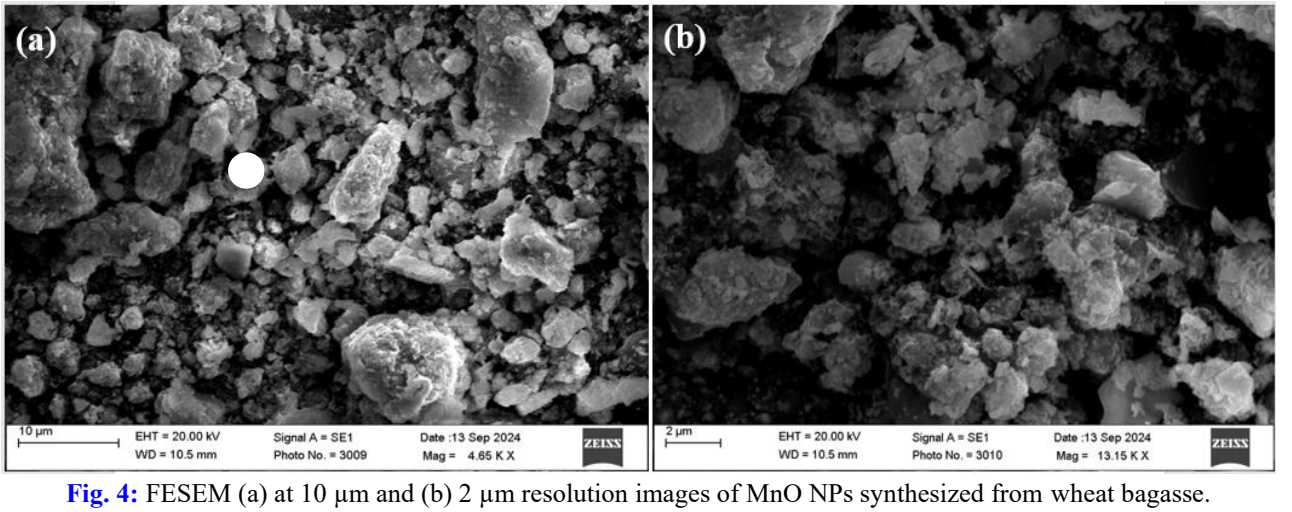

Fig. 4: FESEM (a) at 10 µm and (b) 2 µm resolution images of MnO NPs synthesized from wheat bagasse.

findings of the study of manganese oxide nanoparticles made from wheat bagasse ethanol extract.

3.3 Biological activities

3.3.1 Antioxidant activity

3.3.1.1 DPPH and ABTS free radical scavenging assay

The DPPH radical scavenging test was employed to evaluate the antioxidant capacity of the synthesised MnO NPs. A 0.1 mM solution of DPPH was prepared using methanol, and 1 mL of this solution was combined with 1 mL of a nanoparticle suspension in methanol at varying concentrations (10–30 µg/mL). A UV-Vis spectrophotometer was utilised to measure the absorbance at 517 nm after the mixture was incubated in the dark for thirty minutes. The absorbance of the sample was compared to that of the control (DPPH solution without nanoparticles), using ascorbic acid as a positive control, to determine the level of DPPH scavenging activity. As nanoparticle concentration increased, the radical scavenging activity also increased, indicating a concentration-dependent antioxidant potential.[25] The assessment of DPPH free radical

inhibition was conducted utilising the specified formula.

$$\% \text{ Inhibition} = \frac{A_{control} - A_{sample}}{A_{control}} \times 100$$

$A_{control}$ denotes the absorbance of the DPPH solution in the absence of any treatment. nanoparticles and A_{sample} is the absorbance after the addition of nanoparticles. The results were compared to a standard antioxidant (ascorbic acid) to evaluate the antioxidant action of MnO NPs.

The ABTS test was engaged to assess the antioxidant activity of the synthesised MnO NPs. After mixing a 7 mM ABTS solution combined with 2.45 mM $K_2S_2O_8$ and allowed to equilibrate at ambient temperature overnight in the dark, ABTS radicals were produced.[26] Ethanol was then added to the resultant $ABTS^+$ radical solution was adjusted until its absorbance at 734 nm reached 0.80 ± 0.02. Following that, 3 mL of the $ABTS^+$ was added solution was combined with 1 mL of nanoparticle suspension at different doses (10–200 µg/mL) and incubated for 6 minutes to evaluate the antioxidant potential. Equation The proportion of radical scavenging was determined following the measurement of absorbance at 734 nm.

According to the given graph, the DPPH and ABTS radical scavenging assays were utilised to assess the antioxidant activity properties of MnO NPs and ascorbic acid at doses of 5, 10, 20, and 30, 50 µg/mL. Ascorbic acid demonstrated a potent, concentration-dependent scavenging action in the DPPH experiment; at 5 µg/mL, inhibition was around 23%, but at 30 µg/mL, it exceeded 90%. Although it was less than the norm, MnO NPs also showed a dose-dependent response, going from around 7% at 5 µg/mL to roughly 70% at 30 µg/mL. Ascorbic acid also shown strong scavenging action in the ABTS experiment, increasing from around 20% to over 90% across all tested doses. Significant ABTS radical suppression was shown by MnO NPs, with values rising from about 8% at 5 µg/mL to about 75% at 30 µg/mL. IC_{50} value for DPPH and ABTS was found 30.34 and 34.45 µg/mL for MnO NPs. These findings show that MnO NPs are efficient in both DPPH and ABTS radical systems in a concentration-dependent manner and have notable antioxidant qualities, although somewhat weaker than ascorbic acid. Fig. 5 represents the antioxidant activity of MnO nanoparticles synthesized from wheat bagasse, evaluated using ABTS and DPPH radical scavenging assays.

In the literature, green-synthesized metal oxide nanoparticles often demonstrate a wide range of antioxidant efficiencies depending on their composition and synthesis route. For instance, Sivakumar Saipraba *et al*. (2025) reported biogenic Ag–ZnO nanoparticles synthesized using *Andrographis macrobotrys*, which exhibited notable antioxidant activity with IC_{50} values of 85.67 µg/mL and 93.78 µg/mL in DPPH and ABTS assays, respectively.[27] These IC_{50} values are considerably lower than those typically reported for plant-derived MnO/MnO_2 nanoparticles, where antioxidant IC_{50} values commonly range from ~200 to 310 µg/mL, indicating stronger radical-scavenging activity for Ag–ZnO systems. The enhanced antioxidant performance of Ag–ZnO nanoparticles has been attributed to synergistic effects between silver and zinc oxide, as well as increased surface reactivity.[27]

In contrast, MnO nanoparticles synthesized via green routes generally exhibit moderate antioxidant potency but offer distinct advantages related to their redox flexibility and biocompatibility, which may contribute to sustained biological effects beyond single-assay radical scavenging. Overall, these comparisons position the antioxidant activity of the present MnO nanoparticles within the expected range of biogenic MnO systems while highlighting compositional differences relative to other plant-mediated metal oxide nanoparticles.

Comparable trends have also been reported for other plant-mediated metal oxide nanoparticles. Azhagu Madhavan Sivalingam et al. investigated ZnO nanoparticles synthesized using *Avicennia marina* extract and demonstrated strong, dose-dependent antioxidant and antimicrobial activities. At a concentration of 100 µg/mL, the AM–ZnO nanoparticles exhibited radical scavenging efficiencies of 23.12 % (hydroxyl), 15.12 % (ABTS), 14.15 % (superoxide), and 14.05 % (DPPH), indicating notable antioxidant potential. In addition, the nanoparticles showed significant antibacterial activity with inhibition zones of 19.5 mm against *Pseudomonas aeruginosa*, 16.8 mm against *Staphylococcus aureus*, 16.9 mm against *Klebsiella pneumoniae*, and 14.3 mm against *Salmonella typhi*, along with antifungal activity against *Fusarium graminearum*, *Alternaria alternata*, and *Candida albicans*. When compared with such ZnO-based systems, biogenic MnO nanoparticles generally exhibit moderate antioxidant potency with higher IC_{50} values but benefit from manganese's multiple oxidation states, which can support sustained redox activity and biological interactions. These comparisons highlight that while ZnO nanoparticles often display stronger immediate radical scavenging and antimicrobial effects, MnO nanoparticles synthesized via green routes remain competitive and biologically relevant within the broader class of agro-waste-derived metal oxide nanoparticles.[28]

3.3.2 Antidiabetic activity

3.3.2.1 The α-glucosidase and α-amylase inhibitory activity

As per given graph, MnO NPs' antidiabetic effectiveness was evaluated using α-glucosidase and α-amylase inhibition tests, and contrasted with that of the common medication ascorbic acid at doses of 20, 50, 100, 250 and 300 µg/mL. The findings show that ascorbic acid and MnO NPs both exhibit concentration-dependent increases in enzyme inhibition. MnO NPs shown a progressive increase in activity in the α-amylase inhibition test, with IC_{50} value 256.45 µg/mL and 84.29 µg/mL for Acarbose. Similarly, MnO NPs shown increasing inhibitory capability in the α-amylase inhibition experiment, IC_{50} value was found 215.76 µg/mL and 78.51 µg/mL for ascorbic acid. According to these results, MnO NPs may be a natural antidiabetic drug since they have strong inhibitory effect against the α-amylase and α-glucosidase enzymes. Fig. 6

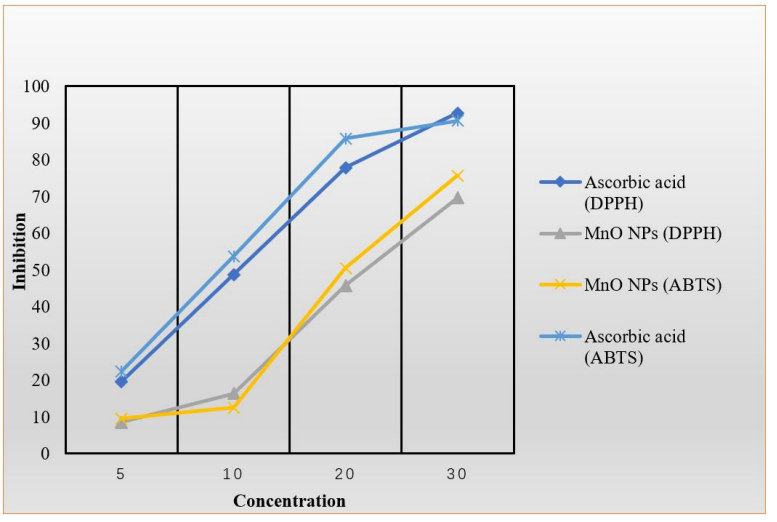

Fig. 5: Antioxidant activity by ABTS and DPPH method of MnO NPs synthesized from wheat bagasse.

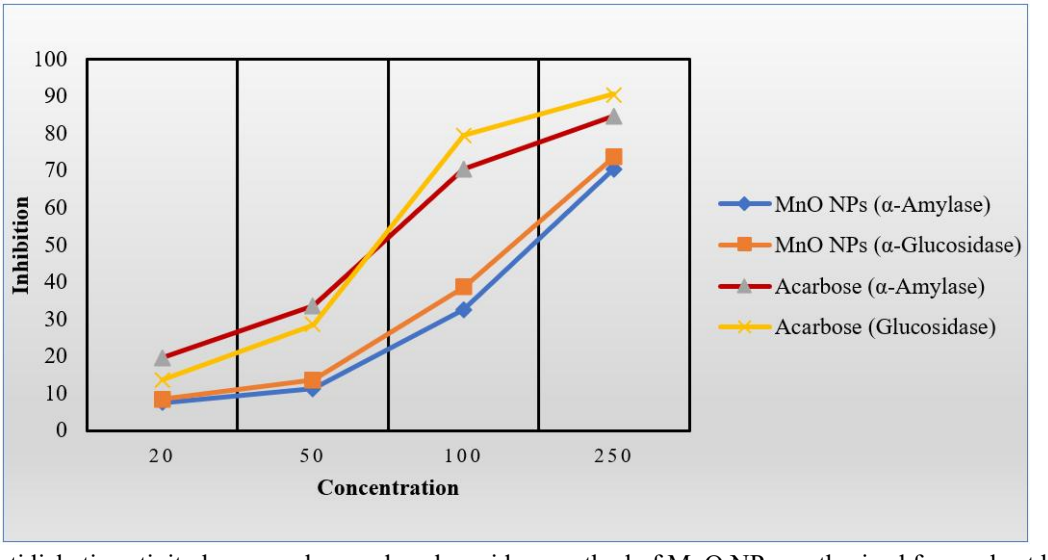

Fig. 6: Antidiabetic activity by α-amylase and α-glucosidase method of MnO NPs synthesized from wheat bagasse.

represents the antidiabetic activity of MnO nanoparticles synthesized from wheat bagasse, evaluated using α-amylase and α-glucosidase inhibition assays.

3.3.3 Antimicrobial activity

The antibacterial efficacy of MnO NPs against bacterial species, such as *Listeria monocytogen*, *Staphylococcus aureus*, *Escherichia coli* and *Pseudomonas aeriginosa*, was assessed using the agar well diffusion technique. After being inoculated into nutrient broth, fresh bacterial cultures were cultured for 18 to 24 hours at 37 °C. A positive control was a well with a conventional antibiotic (norfloxacin), while the negative control was a well with sterile distilled water. After one day incubation at room temperature, the zones of inhibition were quantified in millimetres.

The disc diffusion method was utilised to assess the antibacterial effectiveness of ethanolic extract and MnONPs, as shown in Fig. 7. Significant antibacterial activity was shown by MnO NPs, particularly against S. aureus and P. aeruginosa, inhibition zones recorded at 16 mm and 17 mm, respectively, at the highest dose. Because of differences within the composition of their cellular walls, Gram-negative bacteria seem to be more susceptible to MnONPs' antibacterial effects.[29]

Gram-positive bacteria possess multiple layers of peptidoglycan within their cell membrane, which gives them a more solid structure than Gram-negative bacteria, which only have one layer. The findings demonstrated that the MnO nanoparticles had concentration-dependent antibacterial activity, with Gram-negative bacteria showing the strongest inhibition, indicating that they may be useful antimicrobial agents.[30]

3.3.4 Photocatalytic analysis of MnO NPs

Congo red (CR), a representative organic pollutant, was utilised to assess the photocatalytic dye degradation potential of synthesised nanomaterials under visible light exposure.[31] In a beaker, 50 mL of the dye solution was combined with 10 mg of MnO nanoparticles sourced from a stock solution of CR (10 mg/L). A UV-Vis spectrophotometer was employed to

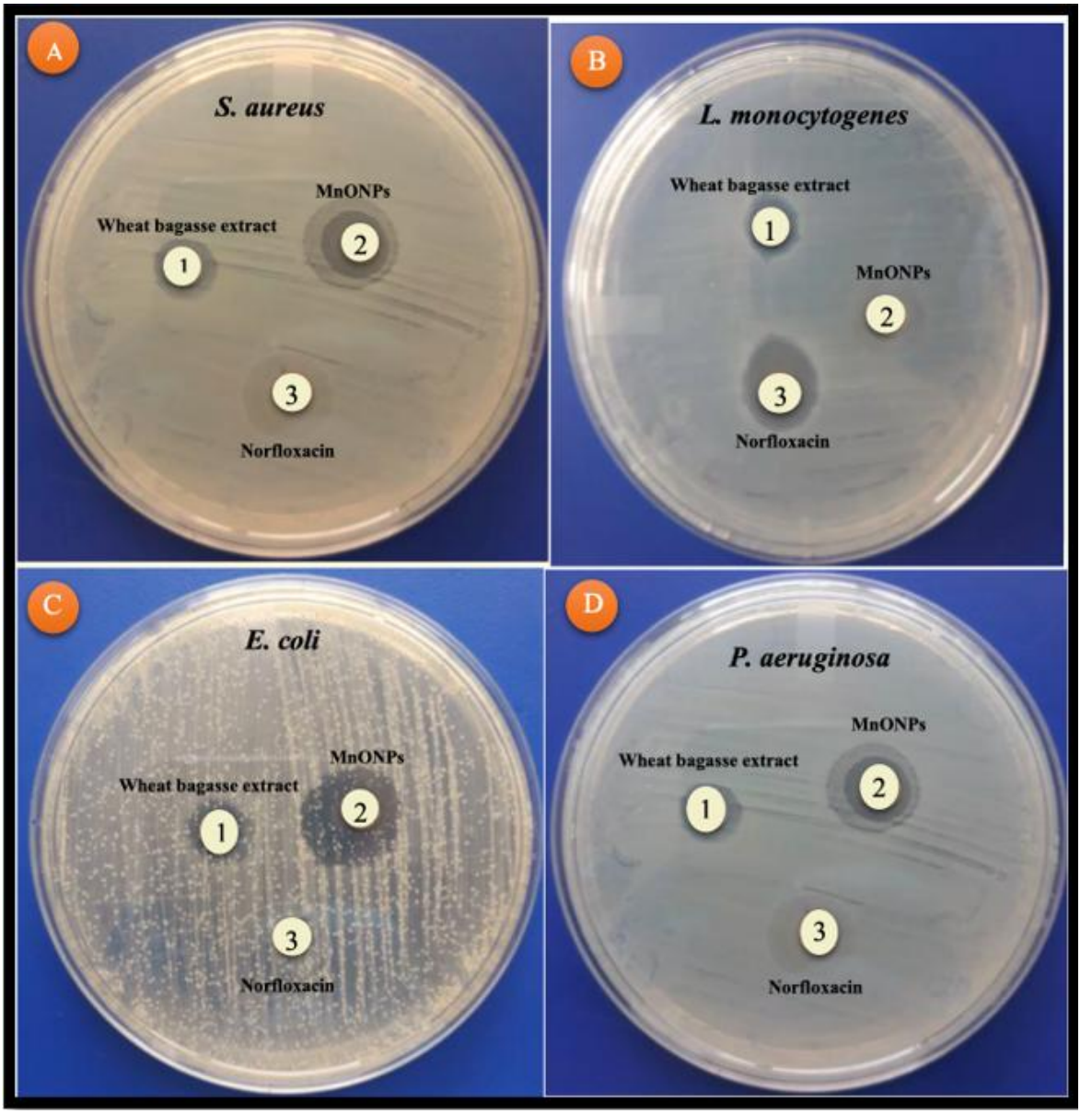

Fig. 7: Antibacterial activity using disc diffusion assay of MnO NPs synthesised from wheat bagasse.

assess the absorbance of the clear supernatant at 664 nm after 3 mLof the solution was periodically removed and centrifuged to eliminate nanoparticles. The degradation efficiency (%) was determined utilising the formula:

$$\text{Degradation (\%)} = \frac{CO - Ct}{Co} \times 100$$

In this context, C_0 denotes the initial absorbance of the dye, while C_t represents the absorbance measured at time t. The MnO nanoparticles' potential in wastewater treatment applications was highlighted by their strong photocatalytic activity, which showed effective degradation of congo red when exposed to visible light.

As shown in Fig. 8, the breakdown of CR dye and the role of MnO NPs as photo-catalysts were demonstrated by the absorption spectra under UV light. The gradual decrease in absorbance at 664 nm suggests that MnO NPs are effectively promoting the degradation process. For MnO NPs, the degradation efficiency over 100 minutes was 85%. Analysing the nanoparticles' surface area, shape, and crystallinity may help explain their photocatalytic activity.[32] Improving the degree of crystallinity and the surface area of the material leads to enhanced photocatalytic performance, subsequently influencing the overall degradation efficiency.[33]

An 85 % degradation efficiency for methylene blue places the synthesized nanoparticles within the upper performance range reported for biogenic photocatalysts. Several green-synthesized ZnO and TiO_2 nanoparticles derived from plant or agricultural waste typically achieve dye degradation efficiencies between 70–95 % under UV or visible light irradiation, depending on catalyst dosage, light source, and reaction time. For example, biogenic Ag–ZnO nanoparticles synthesized using *Andrographis macrobotrys* achieved approximately 85–90 % methylene blue degradation, attributed to the synergistic effect of Ag incorporation and enhanced charge separation. Similarly, plant-mediated ZnO

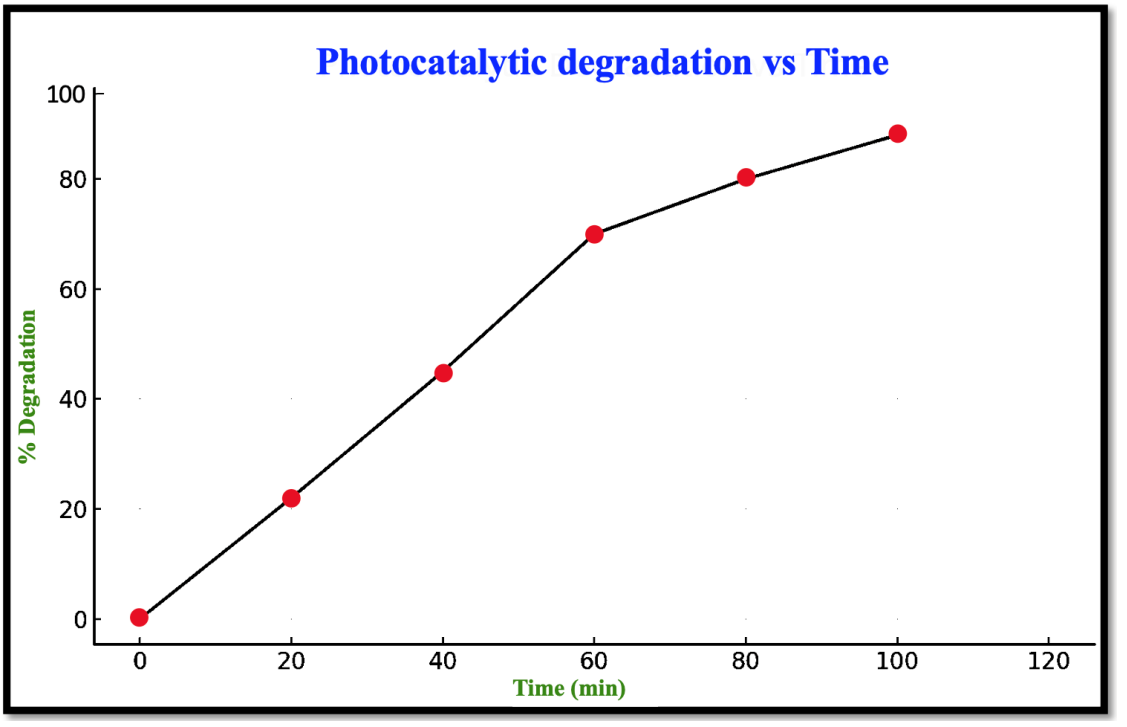

Fig. 8: Analysis of the percentage degradation of irradiation time in relation to Congo red dye when utilising MnO NPs derived from wheat bagasse extract.

nanoparticles reported by Azhagu Madhavan Sivalingam et al. showed degradation efficiencies exceeding 80% for organic dyes under optimized conditions.[34] Compared to TiO_2 nanoparticles synthesized via green routes, which often require longer irradiation times to reach comparable efficiencies, the observed 85 % degradation demonstrates effective photocatalytic performance. While some chemically synthesized or doped systems may exceed 90–95 % efficiency, these often rely on harsher synthesis conditions or noble-metal loading. Therefore, the achieved 85 % dye degradation efficiency is competitive and highlights the effectiveness of green-synthesized nanoparticles as sustainable and efficient photocatalysts.[35]

The present study provides a sustainable approach for synthesizing manganese oxide nanoparticles (MnO NPs) utilizing wheat bagasse extract, highlighting the valorization of agricultural waste within a green chemistry framework. Wheat bagasse, rich in polyphenols, flavonoids, and other reducing biomolecules, efficiently assisted the bioreduction and stability of MnO nanoparticles, as indicated by spectroscopic and microscopic characterization.[36] The development of crystalline MnO and nanoscale morphology demonstrates the potential of wheat bagasse as a low-cost, eco-friendly precursor for nanoparticle synthesis. Compared with conventional chemical approaches, this biogenic technology lowers harmful chemicals while giving enhanced environmental compatibility.[37] The biological activities of the produced MnO NPs, including antioxidant, antidiabetic, and antibacterial properties, demonstrated concentration-dependent behavior, comparable with previous results on plant-mediated metal oxide nanoparticles. These activities may be attributable to the combined impacts of nanoscale size, strong surface reactivity, and surface-bound phytochemicals inherited from the wheat bagasse extract.[38] Their performance is comparable to numerous green-synthesised metal oxide nanoparticles reported in the literature, suggesting potential for early biomedical applications, even if the measured bioactivities were moderate in comparison to standard reference compounds.[39-41] In addition to biological performance, the MnO nanoparticles displayed promising photocatalytic activity toward methylene blue degradation under light irradiation, achieving approximately 85 % elimination efficiency. This behavior is probably caused by the production of reactive oxygen species during photoexcitation, which causes dye molecules to undergo oxidative breakdown.[42] The degradation efficiency compares favorably with other biogenic metal oxide systems, indicating the suitability of wheat bagasse-derived MnO NPs in wastewater treatment and environmental remediation.[43]

Recent studies have demonstrated that green-synthesized metal oxide nanoparticles derived from plant or agricultural waste exhibit promising biological and photocatalytic properties; however, comparative analyses across different metal oxides remain limited. Biogenic ZnO and Ag–ZnO nanoparticles synthesized from plant extracts such as *Andrographis macrobotrys* and *Avicennia marina* have shown strong antioxidant activity with relatively low IC_{50} values and high photocatalytic dye degradation efficiencies, often exceeding 80–90 %, which are attributed to enhanced surface reactivity and synergistic metal effects.[44-46] In contrast, fewer studies have systematically explored biogenic MnO nanoparticles synthesized from agro-waste, particularly with

respect to their antioxidant, antidiabetic, and photocatalytic performance relative to other metal oxides. Available reports indicate that plant-mediated MnO/MnO_2 nanoparticles generally exhibit moderate antioxidant potency but possess distinct redox flexibility arising from multiple manganese oxidation states, which may support sustained biological and environmental applications. Therefore, a focused investigation of MnO nanoparticles synthesized via green routes, combined with contextual comparison to ZnO and TiO_2 based systems, is essential to clarify their relative advantages and expand the scope of sustainable nanomaterials for biomedical and environmental remediation applications.[47] Although green synthesis of MnO nanoparticles using plant or agro-waste-derived extracts has been previously reported, the present study demonstrates novelty through the utilization of wheat bagasse**,** an abundant and underexplored lignocellulosic agro-residue, as a reducing and stabilizing agent. Unlike commonly used leaf, fruit, or flower extracts, wheat bagasse is rich in cellulose, hemicellulose, lignin, and residual phenolic compounds, which provide a distinct chemical environment for nanoparticle nucleation, surface functionalization, and stabilization. This compositional difference contributes to improved sustainability, cost-effectiveness, and alignment with waste-to-wealth and circular economy principles, thereby differentiating wheat bagasse from previously reported plant-based sources.[48]

From a performance perspective, the biological and photocatalytic activities of wheat-bagasse-derived MnO nanoparticles compare favorably with existing biogenic MnO nanoparticle systems. Reported literature indicates that plant-mediated MnO/MnO_2 nanoparticles typically exhibit antioxidant IC_{50} values in the range of ~200–310 µg/mL, reflecting moderate but consistent radical scavenging efficiency. The antioxidant activity observed in the present study falls within this reported range, confirming comparable biological performance relative to previously synthesized MnO nanoparticles. Furthermore, biogenic MnO nanoparticles reported in earlier studies generally achieve dye degradation efficiencies between 70 and 90 % under comparable irradiation and catalyst-loading conditions. The observed ~85 % methylene blue degradation efficiency in this study therefore demonstrates competitive photocatalytic performance**,** comparable to reported MnO systems and approaching the efficiencies of certain green-synthesized ZnO- and TiO_2-based photocatalysts. Collectively, these results highlight that wheat bagasse not only serves as a viable and sustainable precursor for MnO nanoparticle synthesis but also yields nanoparticles with biological and photocatalytic performances consistent with, and in some cases competitive with, existing biogenic MnO nanoparticle systems.[49,50]

4. Conclusion

This work used an eco-conscious and sustainable approach to effectively synthesise MnO NPs using wheat bagasse extract. The production of MnO NPs from wheat bagasse, an agro-waste, which offered a natural supply of phytochemicals that served as stabilising and reducing agents. The development of distinct nanoparticles with nanoscale crystallite size and functional groups suggestive of plant-mediated synthesis was validated by characterisation methods. The dose-dependent scavenging impact of the biologically produced MnO NPs in the DPPH and ABTS tests indicated their notable antioxidant potential. Furthermore, the nanoparticles demonstrated strong antidiabetic potential by concentration-dependently blocking the α-glucosidase and α-amylase enzymes, although marginally less well than the conventional ascorbic acid. Crucially, the MnO NPs demonstrated broad-spectrum antimicrobial action, successfully preventing the development of bacterial strains, indicating that they may have promise as a natural antibacterial agent. Additionally, the nanoparticles demonstrated effective dye degradation, highlighting their potential use in wastewater treatment and environmental remediation. All of these results demonstrate that MnO NPs from wheat bagasse have multimodal bioactivities and may be used as an affordable, sustainable platform for environmental and medicinal applications.

Acknowledgments

The authors express their sincere gratitude to the Department of Chemistry, IFTM University, Moradabad, for providing essential facilities, and to the Central Laboratory at Delhi University, India, for providing all necessary technical support.

Conflict of Interests

The authors declare no competing interests.

Supporting Information

Not applicable.

CRediT Statement

Amrish Kumar, **Shubhangee Agarwal:** Conceptualization. **Shobhna Mishra** and **Sheetal Tyagi:** Data curation, Formal analysis, Investigation. **Amanpreet Kaur:** Validation. **Amrish Kumar**, **Shubhangee Agarwal:** Writing - Original draft. **Man Vir Singh**, **Amanpreet Kaur:** Writing - Review and editing.

References

[1] L. M. Anaya-Esparza, Z. V. la Mora, O. Vázquez-Paulino, F. Ascencio, A. Villarruel-López, Bell peppers (capsicum annum L.) losses and wastes: source for food and pharmaceutical applications, *Molecules*, 2021, **26**, 5341, doi: 10.3390/molecules26175341.

[2] S. I. Hamdallah, R. Zoqlam, P. Erfle, M. Blyth, A. M. Alkilany, A. Dietzel, S. Qi, Microfluidics for pharmaceutical nanoparticle fabrication: The truth and the myth, *International Journal of Pharmaceutics*, 2020, **584**, 119408, doi: 10.1016/j.ijpharm.2020.119408.

[3] G. A. Marcelo, C. Lodeiro, J. L. Capelo, J. Lorenzo, E. Oliveira, Magnetic, fluorescent and hybrid nanoparticles: From

synthesis to application in biosystems, *Materials Science and Engineering: C*, 2020, **106**, 110104, doi: 10.1016/j.msec.2019.110104.
[4] A.-G. Niculescu, C. Chircov, A. M. Grumezescu, Magnetite nanoparticles: Synthesis methods–A comparative review, *Methods*, 2022, **199**, 16-27, doi: 10.1016/j.ymeth.2021.04.018.
[5] M. C. Uribe-López, M. C. Hidalgo-López, R. López-González, D. M. Frías-Márquez, G. Núñez-Nogueira, D. Hernández-Castillo, M. A. Alvarez-Lemus, Photocatalytic activity of ZnO nanoparticles and the role of the synthesis method on their physical and chemical properties, *Journal of Photochemistry and Photobiology A: Chemistry*, 2021, **404**, 112866, doi: 10.1016/j.jphotochem.2020.112866.
[6] N. A. Patil, S. Udgire, D. R. Shinde, P. D.Patil, Green synthesis of gold nanoparticles using extract of Vitis vinifera, Buchananialanzan, Juglandaceae, phoenix dactylifera plants, and evaluation of antimicrobial activity, *Chemical Methodologies*, 2023, 7, 15-27, doi: 10.22034/chemm.2023.355289.1597.
[7] J. S. Boruah, C. Devi, U. Hazarika, P. V. Bhaskar Reddy, D. Chowdhury, M. Barthakur, P. Kalita, Green synthesis of gold nanoparticles using an antiepileptic plant extract: *in vitro* biological and photo-catalytic activities, *RSC Advances*, 2021, **11**, 28029-28041, doi: 10.22034/chemm.2023.355289.1597.
[8] G. Suriyakala, S. Sathiyaraj, R. Babujanarthanam, K. M. Alarjani, D. S. Hussein, R. A. Rasheed, K. Kanimozhi, Green synthesis of gold nanoparticles using Jatropha integerrima Jacq. flower extract and their antibacterial activity, *Journal of King Saud University-Science*, 2022, **34**, 101830, doi: 10.1016/j.jksus.2022.101830.
[9] F. A. Alhumaydhi, Green synthesis of gold nanoparticles using extract of *Pistacia chinensis* and their *in vitro* and *in vivo* biological activities, *Journal of Nanomaterials*, 2022, **2022**, 5544475, doi: 10.1155/2022/5544475.
[10] O. Usman, M. M. Mohsin Baig, M. Ikram, T. Iqbal, S. Islam, W. Syed, M. B. A. Al-Rawi, M. Naseem, Green synthesis of metal nanoparticles and study their anti-pathogenic properties against pathogens effect on plants and animals, *Scientific Reports*, 2024, **14**, 11354, doi: 10.1038/s41598-024-61920-8.
[11] M. Bokolia, D. Baliyan, A. Kumar, R. Das, R. Kumar, B. Singh, Biogenic synthesis of nanoparticles using microbes and plants: mechanisms and multifaceted applications, *International Journal of Environmental Analytical Chemistry*, 2025, **105**, 2069-2097, doi: 10.1080/03067319.2024.2305238.
[12] T. U. Rahman, H. Khan, W. Liaqat, M. A. Zeb, Phytochemical screening, green synthesis of gold nanoparticles, and antibacterial activity using seeds extract of *Ricinus communis* L, *Microscopy Research and Technique*, 2022, **85**, 202-208, doi: 10.1002/jemt.23896.
[13] A. Shukla, A. Kaur, R. K. Shukla, Evaluation of different biological activities of leaves of ehretia acuminata r. br, *Indian Drugs*, 2021, **58**, 42-49, doi: 10.53879/id.58.04.12201.
[14] A. Kaur, M. V. Singh, N. Bhatt, S. Arora, A. Shukla, Exploration of chemical composition and biological activities of the essential oil from ehretia acuminata R. Br. fruit, *ES Food & Agroforestry*, 2023, **15**, 1068, doi: 10.30919/esfaf1068.
[15] A. Shukla, A. Kaur, R. K. Shukla, Anchal, Comparative Evaluation of Antioxidant capacity, Total flavonoid and Phenolic content of *Ehretia acuminata* R. Br. fruit, *Research Journal of Pharmacy and Technology*, 2019, **12**, 1811, doi: 10.5958/0974-360x.2019.00302.0.
[16] A. Kaur, A. Shukla, R. K. Shukla, *In vitro* antidiabetic and anti-inflammatory activities of the bark of *Ehretia acuminata* R.Br, *Indian Journal of Natural Products and Resources*, 2022, 538-543, doi: 10.56042/ijnpr.v12i4.29108.
[17] P. Pokhriyal, A. Kaur, A. Shukla, S. Dhiman, H. Gupta, Biocompatible zinc nanoparticles synthesis from ficus subincisa for a sustainable tomorrow: characterization and therapeutic applications, *Russian Journal of Bioorganic Chemistry*, 2024, **50**, 408-417, doi: 10.1134/S1068162024020158.
[18] A. Fouda, A. M. Eid, E. Guibal, M. F. Hamza, S. E. Hassan, D. H. M. Alkhalifah, D. El-Hossary, Green synthesis of gold nanoparticles by aqueous extract of zingiber officinale: characterization and insight into antimicrobial, antioxidant, and *in vitro* cytotoxic activities, *Applied Sciences*, 2022, **12**, 12879, doi: 10.3390/app122412879.
[19] S. Ahmad Khan, S. Shahid, C.-S. Lee, Green synthesis of gold and silver nanoparticles using leaf extract of clerodendrum inerme; characterization, antimicrobial, and antioxidant activities, *Biomolecules*, 2020, **10**, 835, doi: 10.3390/biom10060835.
[20] B. Boro, J. S. Boruah, C. Devi, Alemtoshi, B. Gogoi, P. Bharali, P. V. B. Reddy, D. Chowdhury, P. Kalita, A novel route to fabricate ZnO nanoparticles using Xanthium indicum ethanolic leaf extract: Green nanosynthesis perspective towards photocatalytic and biological applications, *Journal of Molecular Structure*, 2024, **1300**, 137227, doi: 10.1016/j.molstruc.2023.137227.
[21] E. V. Kumar, B. S. Niveditha, L. Sushmitha, B. K. Usha, B. E. Kumara swamy, Anitha, G. Nagaraju, Facile green synthesis of Cu-doped MoO_3 nanoparticles and its application for the photocatalytic degradation of hazardous organic pollutants, *Nano-Structures & Nano-Objects*, 2023, **36**, 101066, doi: 10.1016/j.nanoso.2023.101066.
[22] S. A. Korde, P. B. Thombre, S. S. Dipake, J. N. Sangshetti, A. S. Rajbhoj, S. T. Gaikwad, Neem gum (Azadirachta indicia) facilitated green synthesis of TiO_2 and ZrO_2 nanoparticles as antimicrobial agents, *Inorganic Chemistry Communications*, 2023, **153**, 110777, doi: 10.1016/j.inoche.2023.110777.
[23] F. Barzegarparay, H. Najafzadehvarzi, R. Pourbagher, H. Parsian, S. M. Ghoreishi, S. Mortazavi-Derazkola, Green synthesis of novel selenium nanoparticles using Crataegus monogyna extract (SeNPs@CM) and investigation of its toxicity, antioxidant capacity, and anticancer activity against MCF-7 as a breast cancer cell line, *Biomass Conversion and Biorefinery*, 2024, **14**, 25369-25378, doi: 10.1007/s13399-023-04604-z.
[24] M. Shahbaz, A. Akram, N. I. Raja, T. Mukhtar, A. Mehak, N. Fatima, M. Ajmal, K. Ali, N. Mustafa, F. Abasi, Antifungal activity of green synthesized selenium nanoparticles and their effect on physiological, biochemical, and antioxidant defense system of mango under mango malformation disease, *PLoS One*, 2023, **18**, e0274679, doi: 10.1371/journal.pone.0274679.

[25] Z. Villagrán, L. M. Anaya-Esparza, C. A. Velázquez-Carriles, J. M. Silva-Jara, J. M. Ruvalcaba-Gómez, E. F. Aurora-Vigo, E. Rodríguez-Lafitte, N. Rodríguez-Barajas, I. Balderas-León, F. Martínez-Esquivias, Plant-based extracts as reducing, capping, and stabilizing agents for the green synthesis of inorganic nanoparticles, *Resources*, 2024, **13**, 70, doi: 10.3390/resources13060070.
[26] A. Sati, T. N. Ranade, S. N. Mali, H. K. Ahmad Yasin, A. Pratap, Silver nanoparticles (AgNPs): comprehensive insights into bio/synthesis, key influencing factors, multifaceted applications, and Toxicity─A 2024 update, *ACS Omega*, 2025, **10**, 7549-7582, doi: 10.1021/acsomega.4c11045.
[27] S. Saipraba, R. Meena, C. Ragavendran, M. K. Gatasheh, A. Ahmed, S. Murugesan, Biogenic Ag-ZnO nanoparticles synthesized *via* Andrographis macrobotrys Nees: a dual role in biomedical applications and methylene blue dye degradation, *Next Materials*, 2025, **9**, 101030, doi: 10.1016/j.nxmate.2025.101030.
[28] A. M. Sivalingam, Green synthesis of Avicennia marina-derived ZnO nanoparticles *in vitro* antioxidant and antimicrobial activity, drug genotoxic effects on MCF-7 cells, *Inorganic Chemistry Communications*, 2026, **183**, 115767, doi: 10.1016/j.inoche.2025.115767.
[29] A. Waris, M. Din, A. Ali, M. Ali, S. Afridi, A. Baset, A. Ullah Khan, A comprehensive review of green synthesis of copper oxide nanoparticles and their diverse biomedical applications, *Inorganic Chemistry Communications*, 2021, **123**, 108369, doi: 10.1016/j.inoche.2020.108369.
[30] A. Singh, P. K. Gautam, A. Verma, V. Singh, P. M. Shivapriya, S. Shivalkar, A. K. Sahoo, S. K. Samanta, Green synthesis of metallic nanoparticles as effective alternatives to treat antibiotics resistant bacterial infections: a review, *Biotechnology Reports*, 2020, **25**, e00427, doi: 10.1016/j.btre.2020.e00427.
[31] S. C. Mali, A. Dhaka, C. K. Githala, R. Trivedi, Green synthesis of copper nanoparticles using Celastrus paniculatus Willd. leaf extract and their photocatalytic and antifungal properties, *Biotechnology Reports*, 2020, **27**, e00518, doi: 10.1016/j.btre.2020.e00518.
[32] S. Ying, Z. Guan, P. C. Ofoegbu, P. Clubb, C. Rico, F. He, J. Hong, Green synthesis of nanoparticles: Current developments and limitations, *Environmental Technology & Innovation*, 2022, **26**, 102336, doi: 10.1016/j.eti.2022.102336.
[33] A. Kumar, A. Kaur, M. V. Singh, Vinod, S. Dhiman, Rice bagasse extract-based green synthesis of zinc oxide nanoparticles: characterisation, assessment of anti-skin cancer, antibacterial, and antioxidant properties, *Sustainable Chemistry for Climate Action*, 2025, **7**, 100118, doi: 10.1016/j.scca.2025.100118.
[34] S. Gupta, A. Kaur, M. V. Singh, D. Rana, K. Nandan, Y. Kumar, S. Sharma, A. Chauhan, S. K. Verma, Biosynthesis of silver nanoparticles using raphanus sativus ethanolic leaf extract and their photocatalytic degradation of dyes from polluted water and biological activities, *ES Food & Agroforestry*, 2025, **23**, 1953, doi: 10.30919/faf1953.
[35] K. Bano, S. Kaushal, A. Kumar, P. P. Singh, Sunlight-driven photocatalytic degradation of 4-nitrophenol and adsorptive removal of Mn (II) ions from industrial wastewater by biogenic synthesized CuO/SnO_2 heterojunction, *Materials Today Chemistry*, 2022, **26**, 101193, doi: 10.1016/j.mtchem.2022.101193.
[36] S. Kaushal, A. Kumar, H. Bains, P. P. Singh, Photocatalytic degradation of tetracycline antibiotic and organic dyes using biogenic synthesized CuO/Fe_2O_3 nanocomposite: pathways and mechanism insights, *Environmental Science and Pollution Research*, 2023, **30**, 37092-37104, doi: 10.1007/s11356-022-24848-y.
[37] S. Kaushal, V. Kumari, P. P. Singh, Sunlight-driven photocatalytic degradation of ciprofloxacin and organic dyes by biosynthesized rGO–ZrO_2 nanocomposites, *Environmental Science and Pollution Research*, 2023, **30**, 65602-65617, doi: 10.1007/s11356-023-27000-6.
[38] K. Bano, S. Kaushal, B. Lal, S. K. Joshi, R. Kumar, P. P. Singh, Fabrication of CuO/ZnO heterojunction photocatalyst for efficient photocatalytic degradation of tetracycline and ciprofloxacin under direct Sun light, *Environmental Nanotechnology, Monitoring & Management*, 2023, **20**, 100863, doi: 10.1016/j.enmm.2023.100863.
[39] R. S. Sodhi, P. P. Singh, B. Lal, S. K. Joshi, R. Kumar, Y. Singh, S. Kaushal, Biogenic synthesis of ZnO nanoparticles using Polystichum squarrosum extract and its applications as anti-oxidant, anti-diabetic agent and industrial waste water treatment, *Emergent Materials*, 2024, **7**, 285-298, doi: 10.1007/s42247-023-00589-7.
[40] V. Kumar, Y. Singh, S. Kaushal, R. Kumar, Bioinspired synthesis of copper oxide nanoparticles using aqueous extracts of Cladophora glomerata (L.) Kuetz and their potential biomedical applications, *Bioprocess and Biosystems Engineering*, 2025, **48**, 633-646, doi: 10.1007/s00449-025-03133-5.
[41] A. Sharma, K. Verma, S. Kaushal, R. Badru, Selective N-alkylation of amines with DMC over biogenic Cu-Zr bimetallic nanoparticles, *ACS Omega*, 2021, **6**, 15300-15307, doi: 10.1021/acsomega.1c01633.
[42] V. Thangapushbam, S. Sivakami, P. Rama, M. Jothika, K. Muthu, A facile green synthesis of Ag@MnO_2 nanoparticles using Martynia annua plant extract and their biological activity and catalytic reduction of dye, *Results in Chemistry*, 2024, **7**, 101495, doi: 10.1016/j.rechem.2024.101495.
[43] C. Bharti, A. Singh, K. Nandan, Vidivay, S. Baghel, Antibacterial and cytotoxic efficacy of Ag–MnO_2/PIn nanocomposites derived from battery waste, *Materials Chemistry and Physics*, 2025, **333**, 130305, doi: 10.1016/j.matchemphys.2024.130305.
[44] A. K. Tiwari, A. K. Singh, S. Jha, S. K. Tripathi, R. R. Awasthi, S. K. Mishra, R. P. Ojha, A. K. Bhardwaj, A. Dikshit, Green synthesis of TiO_2 nanoparticles using Kinnow peel extracts and their antioxidant properties, *Scientific Reports*, 2025, **15**, 38307, doi: 10.1038/s41598-025-22078-z.
[45] V. P. Aswathi, S. Meera, C. G. Ann Maria, M. Nidhin, Green synthesis of nanoparticles from biodegradable waste extracts and their applications: a critical review, *Nanotechnology for*

Environmental Engineering, 2023, **8**, 377-397, doi: 10.1007/s41204-022-00276-8.
[46] D. Kalaimurugan, K. Lalitha, K. Durairaj, P. Sivasankar, S. Park, K. Nithya, M. S. Shivakumar, W.-C. Liu, B. Balamuralikrishnan, S. Venkatesan, Biogenic synthesis of ZnO nanoparticles mediated from Borassus flabellifer (Linn): antioxidant, antimicrobial activity against clinical pathogens, and photocatalytic degradation activity with molecular modeling, *Environmental Science and Pollution Research*, 2022, **29**, 86308-86319, doi: 10.1007/s11356-021-18074-1.
[47] S. Balasubramaniyam, T. Rathinam, M. Srinivasan, P. Arulselvan, S. Mickymaray, F. A. Alfaiz, Green-engineered synthesis of zinc oxide (ZnO) nanoparticles using Musa paradisiaca: evaluation of antioxidant, antimicrobial, anti-inflammatory, and antihyperglycemic activities, *3 Biotech*, 2025, **15**, 358, doi: 10.1007/s13205-025-04526-9.
[48] S. Gupta, A. Kaur, N. Bhatt, M. V. Singh, M. Rani, S. Agarwal, Green synthesis of silver nanoparticles using raphanus sativus water extract for enhanced antimicrobial and photocatalytic activities, *Asian Journal of Chemistry*, 2025, **37**, 2773-2780, doi: 10.14233/ajchem.2025.33973.
[49] V. Verma, M. Al-Dossari, J. Singh, M. Rawat, M. G. M. Kordy, M. Shaban, A review on green synthesis of TiO_2 NPs: photocatalysis and antimicrobial applications, *Polymers*, 2022, **14**, 1444, doi: 10.3390/polym14071444.
[50] Y. Tamilselvi, K. Sivasubramanian, L. Lingeshwaran, P. Velmurugan, A. Sureshbabu, V. D. Teja, K. Kumar, J. R. Livingstone, A. S. Selvaraj, D. Daisy, S. Rajkumar, Eco-friendly synthesis of titanium dioxide nanoparticles from Cocos nucifera for improved photocatalytic and antimicrobial applications, *Discover Nano*, 2026, **21**, 4, doi: 10.1186/s11671-025-04426-0.

Publisher's Note: Engineered Science Publisher remains neutral with regard to jurisdictional claims in published maps and institutional affiliations.